



Deposited via The University of York.

White Rose Research Online URL for this paper:

<https://eprints.whiterose.ac.uk/id/eprint/105454/>

Version: Published Version

Article:

Yang, Lei and Pasley, John (2016) Particle-in-cell simulations of hot electron generation using defocused laser light in cone targets. *Physics of Plasmas*. 082705. ISSN: 1089-7674

<https://doi.org/10.1063/1.4961080>

Reuse

Items deposited in White Rose Research Online are protected by copyright, with all rights reserved unless indicated otherwise. They may be downloaded and/or printed for private study, or other acts as permitted by national copyright laws. The publisher or other rights holders may allow further reproduction and re-use of the full text version. This is indicated by the licence information on the White Rose Research Online record for the item.

Takedown

If you consider content in White Rose Research Online to be in breach of UK law, please notify us by emailing eprints@whiterose.ac.uk including the URL of the record and the reason for the withdrawal request.

Particle-in-cell simulations of hot electron generation using defocused laser light in cone targets

Lei Yang and John Pasley

Citation: *Physics of Plasmas* **23**, 082705 (2016); doi: 10.1063/1.4961080

View online: <http://dx.doi.org/10.1063/1.4961080>

View Table of Contents: <http://scitation.aip.org/content/aip/journal/pop/23/8?ver=pdfcov>

Published by the [AIP Publishing](#)

Articles you may be interested in

[Three dimensional particle-in-cell simulations of electron beams created via reflection of intense laser light from a water target](#)

Phys. Plasmas **23**, 043111 (2016); 10.1063/1.4945739

[Effect of defocusing on picosecond laser-coupling into gold cones](#)

Phys. Plasmas **21**, 012702 (2014); 10.1063/1.4861375

[Two-dimensional particle-in-cell simulations of plasma cavitation and bursty Brillouin backscattering for nonrelativistic laser intensities](#)

Phys. Plasmas **13**, 083103 (2006); 10.1063/1.2244528

[Laser light and hot electron micro focusing using a conical target](#)

Phys. Plasmas **11**, 3083 (2004); 10.1063/1.1735734

[Particle-in-cell simulations of Raman laser amplification in preformed plasmas](#)

Phys. Plasmas **10**, 4848 (2003); 10.1063/1.1625940



COMPLETELY REDESIGNED!

PHYSICS TODAY

Physics Today Buyer's Guide
Search with a purpose.

Particle-in-cell simulations of hot electron generation using defocused laser light in cone targets

Lei Yang^{1,2,a)} and John Pasley³

¹Institute of Materials, China Academy of Engineering Physics, P.O. Box 9071, Mianyang 621907, People's Republic of China

²Institute for Fusion Theory and Simulation, Zhejiang University, Hangzhou 310027, China

³York Plasma Institute, Department of Physics, University of York, York YO10 5DD, United Kingdom

(Received 11 April 2016; accepted 2 August 2016; published online 15 August 2016)

The effects of defocusing a high intensity pulse of laser light on the generation of hot electrons in a cone are investigated using particle-in-cell simulations. The results indicate that defocused laser light can soften the electron energy spectrum and increase the coupling efficiency compared to the use of a laser in tight focus. It is shown that this is a consequence of the density profile of plasma produced by the laser prepulse, which is less dense in the case of the defocused laser. The relevance of this result to fast ignition inertial confinement fusion is discussed. *Published by AIP Publishing.*
[\[http://dx.doi.org/10.1063/1.4961080\]](http://dx.doi.org/10.1063/1.4961080)

I. INTRODUCTION

Fast ignition inertial confinement fusion is a promising scheme which aims to release energy by nuclear fusion.^{1–3} In the past two decades, there have been many theoretical and experimental investigations performed to explore the suitability of this approach. However, the success of this scheme relies on the production of hot electrons and energy transfer from laser light to the dense imploded fusion fuel. Many methods have been explored to increase the coupling efficiency. In one approach, a gold cone is used to assist the laser in propagating within a short distance of the dense fuel, avoiding the laser light having to propagate through a significant depth of plasma before it interacts with the fuel.⁴

There are several issues which may impact the effectiveness of using a cone in fast ignition. The laser prepulse, caused by amplified spontaneous emission, can cause significant deposition of energy in the cone prior to the arrival of the high intensity laser light. This prepulse is typically of nanosecond duration and may contain as much as 10^{-4} of the energy of the main pulse. As a result, the inner surface of the cone may be ionized by the laser prepulse and filled with preplasma. It is observed that this preplasma can fill the cone to a depth of around $100\ \mu\text{m}$ (Refs. 5–7) using sub-ignition-scale lasers. The presence of this preplasma can severely degrade the coupling efficiency between of main pulse and the cone tip.

A number of schemes have been considered to try and resolve this problem. Some of these look at reducing the amount of energy in the laser prepulse via technological improvements in the laser chain.⁸ However, removing the prepulse entirely may not always be feasible or economic. The idea that is considered in this manuscript is that of changing the focus position of laser light and so reducing the laser intensity at the cone-wall. Doing this also impacts on the hot electron spectrum produced during the interaction. This change in the electron spectrum's characteristic

temperature is also of interest since another difficulty in fast ignition is that the electrons can tend to be too hot to facilitate efficient coupling to the fuel. Another factor to consider is how the efficiency of energy coupling from laser to the fuel changes as the laser is defocused. Following Ref. 9, it was shown experimentally that the electron spectrum is softened in defocus while coupling is approximately maintained. In this paper, we will try and explain this result further using particle-in-cell (PIC) simulations of the interaction of defocused laser light with cone targets.

Simulations using a two-dimensional three-velocity particle-in-cell code have been performed exploring a range of different focus positions in a cone target. The electron energy spectrum, distribution of divergence angle, effective location of emission, and the energy coupling efficiency are evaluated. It is observed that the hot electron energy spectra are softened when using defocused laser pulse, as shown in Ref. 9; in addition, the coupling efficiency is increased as well.

II. SIMULATION SETUP

A 2D3V particle-in-cell (PIC) code¹⁰ is used to simulate the laser-cone interaction and hot electron production. (In this paper, a collisionless code is sufficient. Due to high energy of hot electrons, the effects of collision basically can be omitted.) The density profile of the preplasma produced by the prepulse of the laser is calculated using the radiation-hydrodynamics code Hyades.¹¹ The focus position of laser light is changed from before the cone tip to beyond it.

A simulation box, with the size of $200\ \mu\text{m} \times 200\ \mu\text{m}$, is employed in all of the PIC simulations performed here. In this box, there are 4000×4000 cells in the whole area, so both the transverse and longitudinal resolution $\Delta x = \Delta y = 0.05\ \mu\text{m}$. Meanwhile, there are 64 electrons and 16 ions in each cell, which is enough to avoid artificial self-heating interfering in the simulations. It has been verified that it makes no significant difference to add more particles than this to the cells in these simulations. The coordinate system

^{a)}Author to whom correspondence should be addressed. Electronic mail: yanglei@caep.cn

and the geometry of the gold cone are shown in Fig. 1. The inner surface of the cone's tip is located at the origin of the coordinate system. The half angle of the cone is 20° , and the conical wall is $20\ \mu\text{m}$ thick. The diameter of the inside of cone's tip is $30\ \mu\text{m}$, and the tip itself has a thickness of $6\ \mu\text{m}$.

The plasma density of the gold cone is assumed to be $20n_c$, where n_c is the critical density. The actual density of the cone can in reality approach $\sim 10^4 n_c$, so the density used in the PIC simulations does not accurately reflect this. It was found that it makes no significant difference to the simulation results to increase the density of cone beyond this point however. As discussed in Refs. 5–7, the long duration prepulse of the laser, which is of the order of ns can produce a preplasma inside the cone, which is of the order of $10^{-2} n_c$ to $10n_c$. This means that when the main pulse arrives, it is going through the preplasma prior to interacting with the denser plasma near the cone tip. Due to the inability of the PIC code to accurately low-intensity interactions over many hundreds of picoseconds, a pre-defined preplasma configuration is used to initialise the PIC simulation. This predefined plasma fills the interior volume of the cone, in order to simulate the effects of the preplasma on the characters of hot electrons generated by the interaction with the main pulse. As presented above, the density profile of the preplasma is calculated by the Hyades radiation hydrodynamics simulation code. A different preplasma profile is calculated using the Hyades code for each defocus position, assuming an identical laser power profile, thereby mimicking what would be seen in an experiment with a given laser pulse. In porting the results from the hydrodynamic code to the PIC code, both the cone and the preplasma are assumed to be initially cold, which is reasonable given that the electron temperatures induced by the laser prepulse are insignificant in comparison to those induced by the high intensity part of the pulse. The PIC code has been tested by Wilks' scaling law¹² with parameters presented above, in order to ensure that the simulation results are physical.

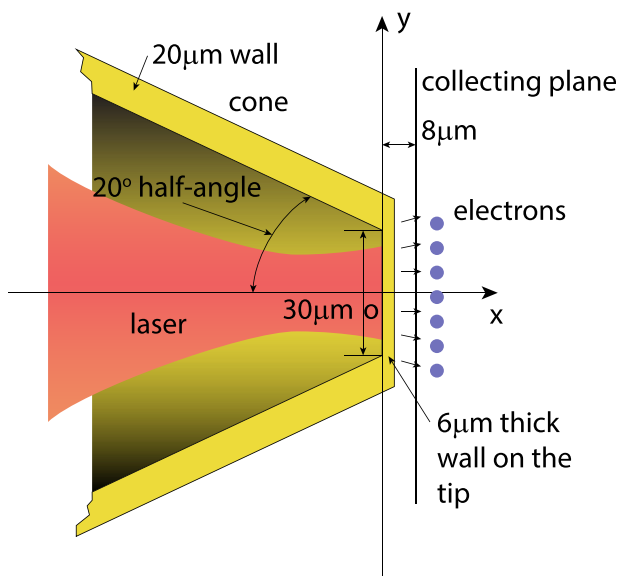


FIG. 1. The coordinate system and geometry of gold cone employed in the simulations.

The laser employed in all these simulations is propagating from left to right towards the center of the cone (as shown in Fig. 1), with a wave-length of $1\ \mu\text{m}$ and an intensity of up to $3 \times 10^{19}\ \text{W}/\text{cm}^2$. The laser beam has a double Gaussian profile, resulting in the high intensity pulse having a duration of 1 ps and a spot size of $8\ \mu\text{m}$ (FWHM) in tight focus. All the relevant parameters of simulations are maintained unchanged for the different focus positions. (The plasma condition of cone is fixed for all simulations, while the preplasma change with laser focus position accordingly.) The focus position is changed from $-800\ \mu\text{m}$ to $800\ \mu\text{m}$, with respect to the inner surface of the cone tip.

III. SIMULATION RESULTS

In order to collect information pertaining to the hot electrons generated by the main pulse, a collecting plane is located $8\ \mu\text{m}$ behind the inner side of tip of the cone (Fig. 1), where electrons are recorded when they pass. As a result, all the spectra of energy and divergence angle are time-integrated, which enables ready comparison with the experiment.

In all the following discussions, the laser with focus position of $0\ \mu\text{m}$ (i.e., the laser is focused on the interior surface of the tip of the cone) is called tight focus; all of the other cases are called defocused. The simulation results show that there is a crucial difference in the hot electrons' character going from tight focus to defocus.

Fig. 2 shows the electron energy density distribution with different laser focus positions. The energy density here is defined as EdN/dE , where E is the energy of electrons and N the number density of electrons. As shown by these 9 curves, the most obvious result is that the energy density curve is substantially broadened in tight focus as compared to the defocused case, and the electron energy is reduced in the defocused case. However, there is not so much of a clear trend between the defocused cases. So, all the defocused cases seem to have a similar effect on the energy distribution of hot electrons. Going from one simulation to another, both the focus position and the profile of the preplasma are

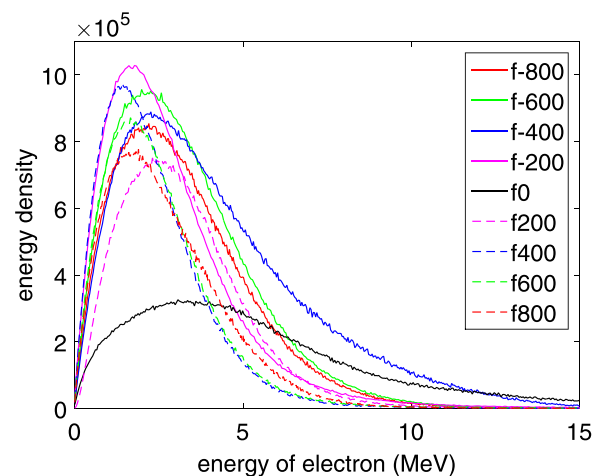


FIG. 2. Electron energy density for the tight focus and defocus cases. The focus positions of all the laser light are $-800\ \mu\text{m}$, $-600\ \mu\text{m}$, $-400\ \mu\text{m}$, $-200\ \mu\text{m}$, $0\ \mu\text{m}$, $200\ \mu\text{m}$, $400\ \mu\text{m}$, $600\ \mu\text{m}$, and $800\ \mu\text{m}$, respectively, represented by the different lines in the figure.

changed in the PIC simulations, so a simple trend is not necessarily to be expected. It should be noted that there is more preplasma produced by the prepulse of the laser in the tight focus case than that in the defocused case and both the presence of this plasma and the higher laser intensity combine to produce the higher electron temperatures seen.

Aside from the energy distribution of the electrons, another interesting quality of the hot electrons produced by the laser light is their divergence angle. This angle is calculated as $\theta = \arctan(|\mathbf{v}_\perp|/|\mathbf{v}_\parallel|)$, where \mathbf{v}_\perp and \mathbf{v}_\parallel are the perpendicular and parallel velocity of electrons along the propagation direction of laser, respectively. As shown in Fig. 3, the divergence angle is smaller in the tight focus case, which is about of 0.5 rad full width (or 28.6°). However, when the defocused laser is used, this divergence angle is increased to approximately 1 rad. This result is obvious because with defocused laser light, the spot size is much larger than when the laser is in tight focus. Therefore, the laser interacts initially with the conical wall, reflecting and scattering, finally resulting in a complicated intensity profile when it interacts with the tip of the cone and produces hot electrons. Consequently, the hot electrons are distributed into a larger region than in the tight focus case. An interesting phenomenon is that the divergence angles split into two directions in the f-400 defocused case, and the emission center is not in the direction of the laser injection.

In order to present the divergence angle distribution for the f-400 case in more detail, the electron energy-density distribution in momentum space is shown in Fig. 4. As one can see from this figure, the electron energy-density is more distributed in two directions, which are around -0.75 rad and 0.5 rad. As mentioned in Ref. 9, when the prepulse hits the cone, the intensity of the laser is much higher at the center of the tip than at the edge. On the other hand, with a higher intensity of illumination, there are more gold atoms ionized into plasma. Therefore, there is more preplasma at the center of the cone. Consequently, when the main pulse arrives, the laser can be concentrated in the area between the cone and the preplasma at the center. As a result, many hot electrons

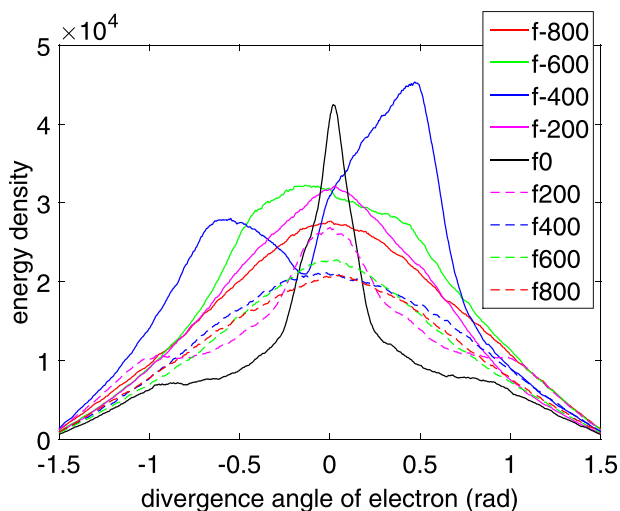


FIG. 3. The distribution of divergence angle of electrons for the different laser focus positions.

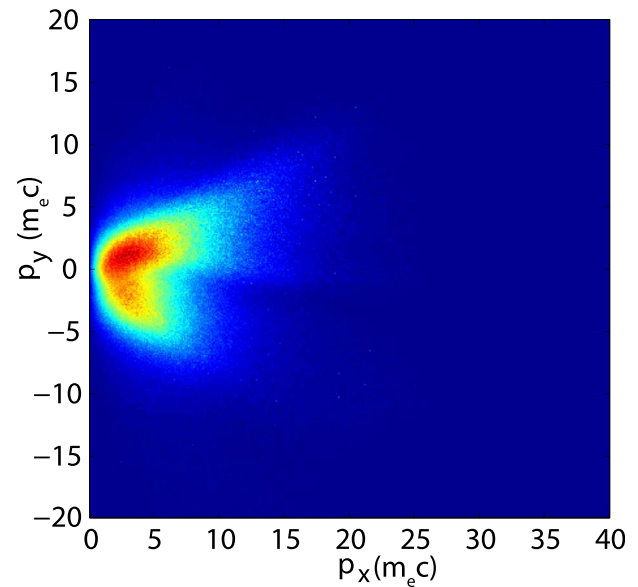


FIG. 4. The electron energy density distribution in momentum space for the f-400 case.

are generated away from the symmetry axis of cone. As for the asymmetrical distribution of divergence angle, this is caused by the asymmetrical reflection of the laser light on either side of the cone, which can be seeded by small non-uniformities. Since such non-uniformities can arise through both physical and non-physical mechanisms in the modeling, it is expected that asymmetries would appear in an experiment but that they may not entirely mirror those seen in a simulation due to the presence of non-physical factors; much as with any PIC simulation of filamentation or other beam-plasma instabilities.

In order to determine the characteristics of hot electrons in the experiment, a wire is used at the end of the cone tip to provide diagnostic emission.⁹ In a fast ignition experiment, this wire is replaced by the fuel. Considering the coupling process of hot electrons with the wire or fuel, therefore, it is also important to know not only the divergence angle but also where the electrons are diverging from. In the present study, the velocity of the diverging electrons is traced backward until it intersects with the axis of the laser, a “virtual focus” point can then be found as the effective location of the emission. Fig. 5 shows the distribution of virtual emission location for the different focusing positions considered.

From Fig. 5, one notes that the virtual emission locations of the hot electrons tend to lie close to the tip of the cone, which means that the majority of the hot electrons seem to be emitted from a region near the tip of the cone. However, the size of this spot changes with the focus position, with the most broad width of about $20 \mu\text{m}$ for the f-400 case and most narrow width of about $6 \mu\text{m}$ for the f-800 case. Therefore, it seems that the focal position of the laser has little to do with the spot size of the emission of hot electrons. Meanwhile, the location of the emission spot (e.g., the effective location of emission) is defined here as a point, on both sides of which there is half of the total electron energy. Naturally, this effective location is changing with the focus position of the laser light, as is shown in Fig. 6.

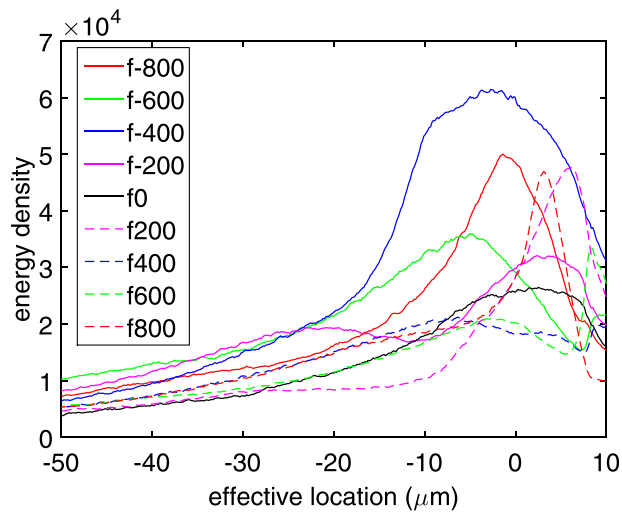


FIG. 5. The distribution of virtual emission location for electrons produced in the different laser focus positions.

The last quantity determining the utility of the hot electrons produced is the coupling efficiency, which is the ratio of the laser energy transferred to electrons. As shown in Fig. 6, it is obvious that the defocused lasers are more efficient than the tight focus laser. (Over 90% of laser energy is reflected by the cone, that is why the coupling efficiency is low.) As mentioned above, as the focus position is changed, the density profile of preplasma is changed as well in the PIC simulations. Therefore, both the focus position and the density profile of preplasma can have an impact upon the coupling efficiency. This result is in keeping with the findings of the experiment; however in the experiment, it was not possible, given the experimental errors, to state conclusively that the coupling was increased in defocus—it was merely observed to be approximately maintained (in itself an interesting result).⁹

All of the results above are diagnosed on the collecting plane located at $x = 8 \mu\text{m}$, which is at the outside of the back of the cone. Therefore, these results can be affected by the sheath field at the edge of the cone. This is acceptable when there is no other material at the end of the cone; however, it is also interesting to investigate what occurs when there is material beyond the cone tip, for example, a wire.⁹ So, Fig. 7

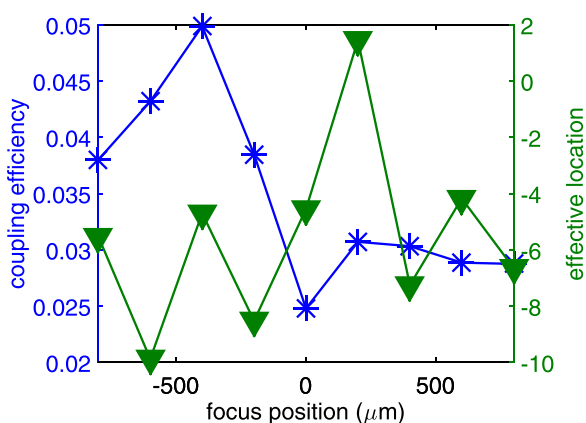


FIG. 6. Energy coupling efficiency and effective emission location for the different focusing positions considered.

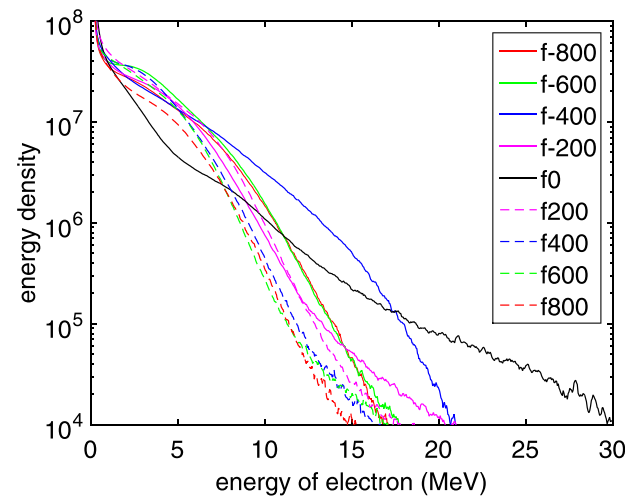


FIG. 7. Electron energy distributions generated in the different focus positions, where the data are collected at a plane inside the cone with $x = 5 \mu\text{m}$.

shows the electron energy distribution again except that now the collecting plane is located inside the cone with $x = 5 \mu\text{m}$. Clearly, the shape of all these curves is totally different from that in Fig. 2, because there are so many cold electrons; however, the basic conclusion is the same. As one can see from the figure, the electrons generated by the tight-focus laser still have higher energy than those generated in the defocused case, which means that defocus still results in a softening of the electron energy spectrum. Again, there is no significant difference among the results for all of the defocused cases, except for similar observations to those mentioned above in respect of the f-400 case.

IV. CONCLUSION

In this paper, the effects of defocusing the high-intensity laser-light irradiating the interior of a gold on the properties of the hot electrons generated are investigated using PIC simulations. The simulation results show that the focus position of the laser light has a significant impact on the electron energy-spectrum, divergence-angle distribution, effective emission location, and energy coupling-efficiency. When the tightly focused laser is used to produce hot electron in a cone, the electron energy spectrum is broadened greatly by the preplasma generated by the prepulse of laser arriving at the cone tip before the main pulse. This preplasma also reduces the coupling efficiency of the laser energy to hot electrons. In contrast, the electron spectrum is softened when using defocused laser light and the coupling efficiency is increased. Therefore, although the tight focus laser displays the smallest hot electron divergence angle, the increased electron temperature and reduced coupling efficiency imply that the effects of preplasma can tend to counter this potential benefit of using a tightly focused laser in fast ignition.

ACKNOWLEDGMENTS

This work was supported by National Natural Science Foundation of China under Grant No. 11505161.

- ¹M. Tabak, J. Hammer, M. E. Glinsky, W. L. Kruer, S. C. Wilks, J. Woodworth, E. M. Campbell, M. D. Perry, and R. J. Mason, *Phys. Plasmas* **1**, 1626 (1994).
- ²J. Nuckolls, L. Wood, A. Thiessen, and G. Zimmerman, *Nature (London)* **239**, 139 (1972).
- ³J. Lindl, *Phys. Plasmas* **2**, 3933 (1995).
- ⁴M. Tabak, J. H. Hammer, E. M. Campbell, W. L. Kruer, J. Goodworth, S. C. Wilks, and M. Perry, Lawrence Livermore National Laboratory Patent Disclosure No. IL8826B (1997).
- ⁵S. D. Baton, M. Koenig, J. Fuchs, A. Benuzzi-Mounaix, P. Guillou, B. Loupias, T. Vinci, L. Gremillet, C. Rousseaux, M. Drouin, E. Lefebvre, F. Dorchie, C. Fourment, J. J. Santos, D. Batani, A. Morace, R. Redaelli, M. Nakatsutsumi, R. Kodama, A. Nishida, N. Ozaki, T. Norimatsu, Y. Aglitskiy, S. Atzeni, and A. Schiavi, *Phys. Plasmas* **15**, 042706 (2008).
- ⁶L. van Woerkom, K. U. Akli, T. Bartal, F. N. Beg, S. Chawla, C. D. Chen, E. Chowdhury, R. R. Freeman, D. Hey, M. H. Key, J. A. King, A. Link, T. Ma, A. J. MacKinnon, A. G. MacPhee, D. Offermann, V. Ovchinnikov, P. K. Patel, D. W. Schumacher, R. B. Stephens, and Y. Y. Tsui, *Phys. Plasmas* **15**, 056304 (2008).
- ⁷R. J. Clarke, D. Neely, R. D. Edwards, P. N. M. Wright, K. W. D. Ledingham, R. Heathcote, P. McKenna, C. N. Danson, P. A. Brummitt, J. L. Collier, P. E. Hatton, S. J. Hawkes, C. Hernandez-Gomez, P. Holligan, M. H. R. Hutchinson, A. K. Kidd, W. J. Lester, D. R. Neville, P. A. Norreys, D. A. Pepler, T. B. Winstone, R. W. W. Wyatt, and B. E. Wyborn, *J. Radiol. Prot.* **26**, 277 (2006).
- ⁸H. Kiriya, T. Shimomura, M. Mori, Y. Nakai, M. Tanoue, S. Kondo, S. Kanazawa, A. S. Pirozhkov, T. Z. Esirkepov, Y. Hayashi, K. Ogura, H. Kotaki, M. Suzuki, I. Daito, H. Okada, A. Kosuge, Y. Fukuda, M. Nishiuchi, M. Kando, S. V. Bulanov, K. Nagashima, M. Yamagiwa, K. Kondo, A. Sugiyama, P. R. Bolton, S. Matsuoka, and H. Kan, *Appl. Sci.* **3**, 214–250 (2013).
- ⁹I. A. Bush, A. G. R. Thomas, L. Gartside, S. Sarfraz, E. Wagenaars, J. S. Green, M. Notley, H. Lowe, C. Spindloe, T. Winstone, A. P. L. Robinson, R. Clarke, T. Ma, T. Yabuuchi, M. Wei, F. N. Beg, R. B. Stephens, A. MacPhee, A. J. MacKinnon, M. H. Key, W. Nazarov, M. Sherlock, and J. Pasley, *Phys. Plasmas* **21**, 012702 (2014).
- ¹⁰Z. M. Zhang, X. T. He, Z. M. Sheng, and M. Y. Yu, *Phys. Plasmas* **18**, 023110 (2011).
- ¹¹J. T. Larsen and S. M. Lane, *J. Quantum Spectrosc. Radiat. Transfer* **51**, 179 (1994).
- ¹²S. C. Wilks, W. L. Kruer, M. Tabak, and A. B. Langdon, *Phys. Rev. Lett.* **69**, 1383 (1992).